

## Simultaneous Electrochemical Preconcentration and Determination of Dopamine and Uric acid by Square-Wave Adsorptive Stripping Voltammetry using a Poly(Safranin O)-Modified Glassy Carbon Electrode

Hayati Filik<sup>1,\*</sup>, Asiye Aslıhan Avan<sup>1</sup>, Sevda Aydar<sup>1</sup>, Rabia Bozdoğan Arpacı<sup>2</sup>

<sup>1</sup>Istanbul University, Faculty of Engineering, Department of Chemistry, 34320 Avcılar Istanbul, Turkey

<sup>2</sup>Mersin University, Medical School, Department of Pathology, 33100 Mersin, Turkey

\*E-mail: [filik@istanbul.edu.tr](mailto:filik@istanbul.edu.tr)

Received: 19 December 2013 / Accepted: 16 February 2014 / Published: 23 March 2014

---

In this paper we present a new method that allows for the simultaneous identification and quantification of dopamine (DA) and uric acid (UA) by square-wave adsorptive stripping voltammetry. Safranin O was electropolymerised on a glassy carbon electrode and then characterised by scanning electron microscopy (SEM), electrochemical impedance spectroscopy (EIS), UV-visible and FT-IR spectroscopy. The electrochemical properties and applications of the modified electrode were studied. In the simultaneous determination of aforementioned two analytes using SW-AdSV, the electrochemical signals were well separated into two oxidation peaks with peak potential differences of 0.176 V (DA–UA). The peaks current are proportional to the concentration of DA and UA over the 0.3–10  $\mu\text{M}$  and 0.5–20  $\mu\text{M}$ . When this modified electrode was used to simultaneously determine DA and UA by SW-AdSV, the detection limits for DA and UA were 0.05  $\mu\text{M}$  and 0.09  $\mu\text{M}$ , respectively. The prepared sensor may be used as a potential sensing platform for detection of DA and UA under coexistence of ascorbic acid. The poly(SFO) modified glassy carbon electrode showed good stability, sensitivity and selectivity. After optimization of analytical conditions, the proposed modified electrode was successfully applied as a sensor for the simultaneous square wave adsorptive stripping voltammetric determination of DA and UA in real human urine samples.

---

**Keywords:** Dopamine, uric acid, safranin O, adsorptive stripping voltammetry, electrochemical sensing, simultaneous determination, serum analysis.

## 1. INTRODUCTION

Dopamine (DA) is a type of monoamine neurotransmitter and hormone, which has a number of important physiological roles in the bodies of humans and animals. A monoamine neurotransmitter that is formed during the synthesis of norepinephrine, it is essential to the normal functioning of the central nervous system [1]. High amounts of dopamine can cause autism, schizophrenia and paranoia. Reduced dopamine concentrations in the brain is associated with the development of Parkinson's disease. In humans, uric acid (UA) is the final oxidative breakdown product of purine nucleotides. High concentrations of UA can cause many diseases, such as gout, hyperuricaemia and Lesch-Nyan disease [5]. In biological fluids, DA concentration is very low (0.01-1  $\mu\text{M}$ ), while the concentration of UA (120  $\mu\text{M}$  to 450  $\mu\text{M}$  ranges) is generally much higher than that of DA [1-6]. Simultaneous detection of these two compounds are a challenge of critical importance not only in the field of biomedical chemistry and neurochemistry but also for diagnostic and pathological research. AA presents in both animal and plant kingdoms, is a vital vitamin in human diet and very popular for its antioxidant properties. A major obstacle in monitoring DA and UA using electrochemical technique is the influence from the coexistence of large amount of AA, since AA can also be oxidized with large over potentials in the result of current overlapping at electrodes [7]. In order to overcome the above-mentioned problems and to improve the selectivity and sensitivity, various electrode-modified materials such as metal nanoparticles, polymers, organic redox mediators, carbon nanofibers, graphene, carbon nanotube and ionic liquid are used [7-33]. AdSV is one of the most sensitive voltammetric techniques, which has been successfully applied for the determination of traces of various compounds [34-36]. The number of compounds analyzed by AdSV has been extended to many biological macromolecules in addition to smaller organic compounds and metal chelates [37,38]. The mercury electrode (hanging mercury drop electrode) is one of the mostly used working electrode in adsorptive stripping voltammetric techniques, another type (nonmercury) of accumulation can be achieved with a chemical interaction between the analyte and the modified electrode surfaces of another (nonmercury) type of working electrode [37-39]. Mercury electrodes have been traditionally employed for achieving high reproducibility and sensitivity of the stripping technique. However, new alternative electrode materials are highly required because of the toxicity of mercury.

Safranine dyes, phenosafranine and safranine (Safranin T and Safranine O) are wellknown diaminophenazine derivatives. Aromatic diamine monomers, including phenosafranine and safranine, were polymerized by chemical oxidation using ammonium persulfate as oxidant [40]. Recently, diaminophenazine derivatives have been electropolymerized by several research groups [40-48]. Aromatic diamine polymers have novel functions in comparison with the common conducting polymers, polyaniline and polypyrrole [49]. Electropolymerization of safranine T on the GCE was constructed by cyclic voltammetry (CV) in phosphate buffer solution. The properties of the resulting polymer [poly(safranine T)] has been characterized, its electrochemical properties investigated, and has been applied to sensors [46-48,50].

The aim of this work is to give a general overview of the reliability and possibility for using nonmercury type electrode for the simultaneous square wave adsorptive stripping voltammetric determination of DA and UA after simultaneous electrochemical preconcentration step. To the best of

our knowledge, no work has been reported on the use of poly(SFO) modified glassy carbon electrode (poly(SFO)/GCE) for the simultaneous square wave adsorptive stripping voltammetric determination of DA and UA after simultaneous electrochemical preconcentration. The poly(SFO)-modified electrode separated the anodic oxidation peak potential of DA and UA with a well-defined peak separation to detect DA and/or UA separately or simultaneously without any intermolecular effects. In addition, the proposed preconcentration method has been applied to simultaneous determination of DA and UA in human urine samples with high selectivity. Adsorptive stripping voltammetry comprises a variety of electrochemical approaches, having a step of pre-concentration onto the electrode surface prior to the voltammetric measurements. Thus, adsorptive stripping analysis is one of the most selective and sensitive voltammetric methods than direct electrochemical methods [7-33].

## 2. EXPERIMENTAL

### 2.1. Apparatus

The voltammetric experiments were performed in an electrochemical assembly with a platinum wire as the counter electrode, a glassy carbon electrode (3 mm diameter) as working electrode and a Ag/AgCl reference electrode. Cyclic voltammetry (CV) experiments were carried out with a Gamry Reference 600 potentiostat (Gamry, USA). All experiments were performed at room temperature (25°C). Before each experiment, the working electrode was polished with a slurry containing 0.3  $\mu\text{m}$  and then with 0.05  $\mu\text{m}$  sized aluminum oxide particles for 5 min. After each treatment, the electrode was washed and ultrasonicated in distilled water for 5 min to remove retained aluminum oxide particles on the electrode surface. The pH values of the solutions were measured by a Hanna HI 221 pH-meter using the full range of 0-14. The acetate buffer was 0.1 mol L<sup>-1</sup> in both CH<sub>3</sub>COOH and CH<sub>3</sub>COONa, while phosphate buffer was prepared from 0.1 mol L<sup>-1</sup> in both phosphoric acid and sodium phosphate. All the other chemicals were analytical grade, or better, and used as received.

### 2.2. Reagents and materials

All chemicals used were of analytical-reagent grade, and distilled water was used throughout. Ascorbic acid, dopamine and uric acid were obtained from Sigma (St. Louis, MO, USA), and they were all used as received. The stock solution of dopamine (1.0  $\times 10^{-2}$  mol L<sup>-1</sup>) (1.0  $\times 10^{-2}$  mol L<sup>-1</sup>) was prepared daily by dissolving dopamine hydrochloride (Merck) in ethanol. Uric acid solution (1.0  $\times 10^{-2}$  mol L<sup>-1</sup>) was prepared by dissolving the solid in a small volume of 1.0  $\times 10^{-2}$  mol L<sup>-1</sup> NaOH solution and diluted to desired concentration with distilled water. Ascorbic acid solution (0.1 mol L<sup>-1</sup>) was prepared by dissolving the solid in distilled water. The solutions were protected from light and stored at 4°C. Before use, all sample solutions were prepared by appropriate dilutions to the desired concentration with distilled water. Safranin O was purchased from Merck and it was used as received. All potentials reported were versus the Ag/AgCl (3.0 M KCl).

### 2.3. Electrode preparation

Before each electrochemical modification, the glassy carbon electrode was first polished with 0.05- $\mu\text{m}$  alumina in a water slurry using a polishing cloth and rinsed with 1:1  $\text{HNO}_3$ , acetone and water, respectively. Poly(safranin O) films were obtained by electrochemical polymerisation, cycling the applied potential from  $-0.8$  to  $1.2$  V vs. Ag/AgCl at scan rate  $50$   $\text{mV s}^{-1}$  in the polymerisation solution containing  $0.5$  mM safranin O. The polymerisation occurred in phosphate buffer solutions at pH 7.0. A uniform film was formed over the entire surface of the GCE after modification. All the resulting modified electrodes were washed with acetate buffer solution (pH 4) before electrochemical measurements. The poly(SFO) modified GCE was stored in acetate buffer solution at pH 4.0.

### 2.4. Analytical procedure

The experiments were conducted in acetate buffer ( $0.1$  M, pH 4.0) at room temperature. All cyclic voltammetric tests were carried out with a scan rate of  $50$   $\text{mV s}^{-1}$  unless otherwise stated. The preconcentration step was carried out at  $-0.2$  V for  $300$  s while stirring the solution. After a  $20$  s equilibration period, the voltammograms were recorded by applying a potential scan from  $0.2$  to  $0.7$  V (with the parameters of step size,  $8$  mV; pulse size,  $75$  mV; frequency,  $10$  Hz, accumulation potential  $-0.2$  V and accumulation time  $300$  s ).

## 3. RESULTS AND DISCUSSION

### 3.1. Morphology images of bare GCE and poly(SFO) modified GCE

Two different electrodes, the bare GCE and poly(SFO) modified GCE, were compared by SEM. The SEM images were randomly captured at different locations of the electrode surface. Fig. 1 shows the SEM images obtained from GCEs modified without/with poly(SFO) thin film. Compared with the glazed surface of bare GCE, the poly(SFO) film has rather featureless fragmental morphology[40].

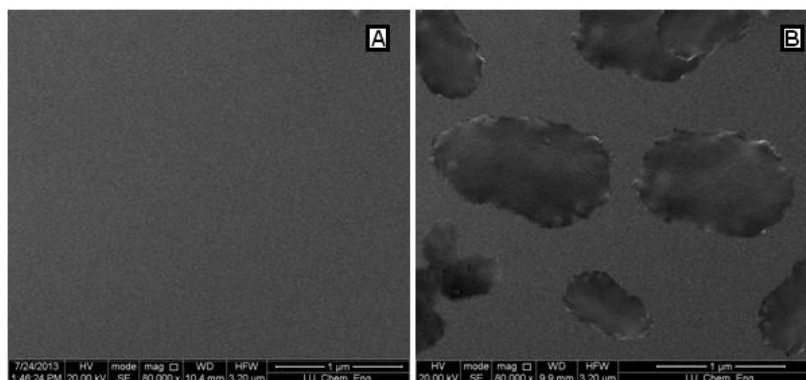


**Figure 1.** The SEM images obtained from GCE without (A)/with (B) poly(SFO) film.

### 3.2. Electrochemical characterization of modified electrodes

The structure of poly(SFO) is discussed on the basis of FT-IR and visible spectra. In the high frequency IR region, the monomer spectrum shows bands at 3439 and 3379  $\text{cm}^{-1}$ , corresponding to the free N-H stretching absorption of primary amino groups and strong, broad bands at 3293 and 3010  $\text{cm}^{-1}$  due to the stretching vibrations of N-H bonds involved in hydrogen bonding. As shown in Fig. 2, the IR spectrum of the polymer shows the characteristic bands at 3400, 3200, and 1610  $\text{cm}^{-1}$  for the amino groups, 1645  $\text{cm}^{-1}$  for the C=N bond, and 1322  $\text{cm}^{-1}$  for C-N bond in poly(safranin O). The 3209 and 1615  $\text{cm}^{-1}$  bands may be assigned to vibrations of primary amino groups  $-\text{NH}_2$ . The 3410  $\text{cm}^{-1}$  band did not allow us to distinguish the secondary amino group  $-\text{NH}-$  from the primary one. The polymer (poly(SFO)) was dissolved in tetrahydrofuran (THF). As a comparison to the electrochemical behavior, the visible absorption spectra of the SFO and poly(SFO) system were performed under the same conditions. The Uv-vis spectrum of a poly(SFO) film showed an absorption maximum at 519 nm in THF. As can be seen in Fig. 3 the absorbance peak position is the same for both the monomer and the polymer. Moreover, under the above conditions the maximum absorption wavelength did not shift, as there was no appearance of any new absorption peak. This means that the monomer chromophores are preserved as the main chromophores in the polymer chains.

The capability of electron transfer on these electrodes was investigated by electrochemical impedance experiments. EIS was often used to monitor the assembly process. Potassium ferricyanide was selected as a probe to estimate the performance of the proposed electrodes. Fig. 4 showed the EIS of different electrodes in 1.0 mM  $\text{Fe}(\text{CN})_6^{3-/4-}$  solution (1:1): bare GCE (Fig. 4a), poly(SFO)/GCE (10 cycles) (Fig. 4b) and poly(SFO)/GCE(20 cycles) (Fig. 4c). It can be seen that a small well-defined semi-circle at higher frequencies was obtained at the bare GCE, indicating small interface electron resistance ( $R_{\text{et}}$ ).

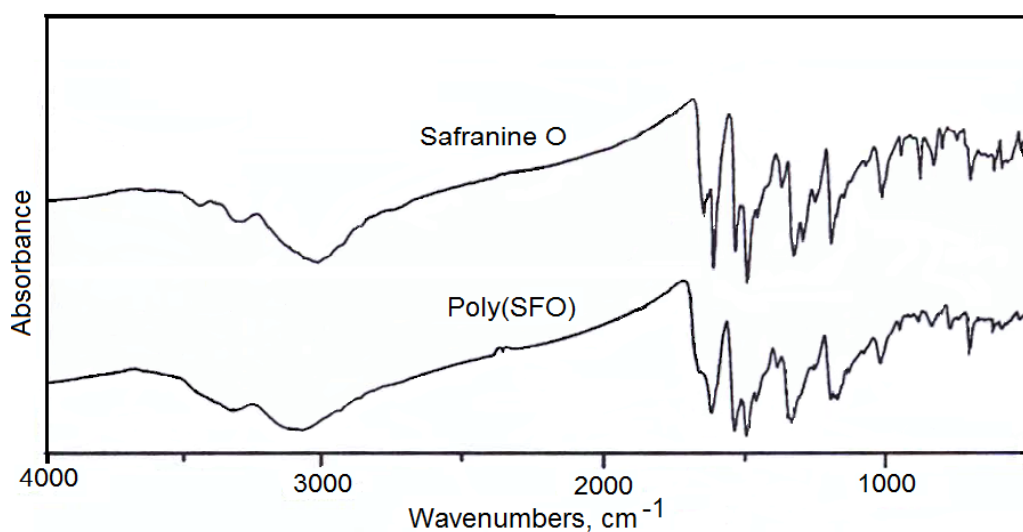


**Figure 2.** FT-IR spectra of safranin O and poly(SFO).

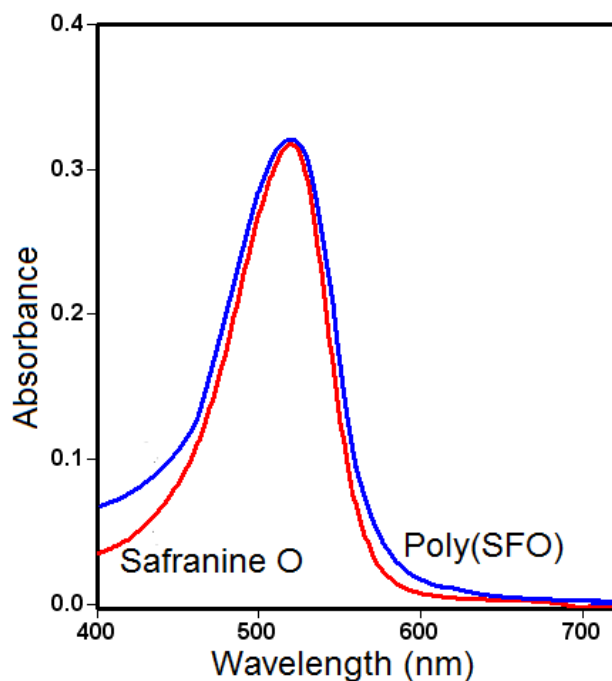


**Figure 3.** UV-vis spectra of safranin O and poly(SFO) in THF.

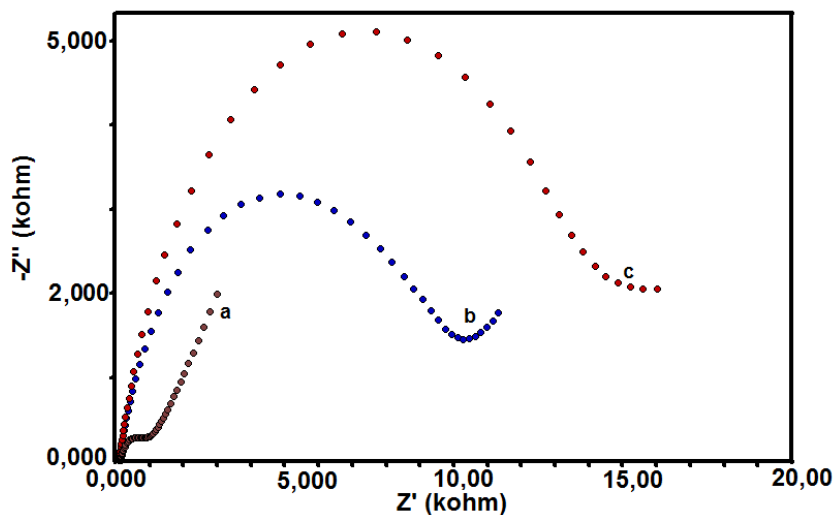


**Figure 4.** Nyquist plots of EIS obtained at (a) bare GCE, (b) poly(SFO) (10 cycles)/GCE and (c) Poly(SFO) (20 cycles)/GCE in 1.0 mM  $\text{Fe}(\text{CN})_6^{3-/4-}$  solution (1:1). EIS condition: frequency range: 100 kHz–0.01 Hz; potential: 0.245 V; perturbation amplitude: 5 mV.

When poly(SFO) film was electrodeposited on the GCE surface (curve b and c), the semi-circle dramatically increased, suggesting that the poly(SFO) film acted as an insulating layer and barriers which made the interfacial charge transfer inaccessible. The diameter of the semi-circle at the high frequency increased along with the electropolymerisation cycles. After fitting suitable circuit and calculation,  $R_{et}$  was obtained as  $948 \pm 0.5 \Omega$ ,  $10170 \pm 0.5 \Omega$  and  $14780 \pm 0.5 \Omega$  for GCE,

poly(SFO)/GCE (10 cycles) and poly(SFO)/GCE (20 cycles), respectively. This result indicated that poly(SFO) film was successfully immobilized on the GCE surface just as designed.

### 3.3. Electrochemical oxidation of DA and UA

The electrochemical behaviors of DA and UA in a mixture solution were studied. Fig. 5 depicts the CVs of DA and UA at the bare and poly(SFO)-modified GCE in 0.1 M acetate buffer (pH 4.0) solution containing 0.1 mM DA and 0.1 mM UA. Fig. 5 (curve c) shows the typical cyclic voltammograms (CVs) of DA and UA at the bare GCE. As can be seen in Fig. 5 (curve c), DA and UA show broader oxidation peaks with the peak potentials at 0.437 mV and 0.653 mV, respectively. When poly(SFO)-modified GCE was used, the mixed biomolecules display two well-resolved oxidation peak from each other, with the oxidation peak potential at ca. 0.417 V for DA and 0.555 V for UA (Fig. 5 curve d). The separation of the cyclic voltammetry peak potentials for DA–UA is about 138 mV. The larger separation of the peak potentials allows selectively determining DA or UA in the presence of the other two species, or simultaneously detecting them in their mixture. In addition, the enhanced peak signal intensity and the lowered overpotential clearly indicate that poly(SFO)-modified GCE has strong electrocatalytic capability towards the target biomolecules. As can be seen in Fig. 5 the background current of poly(SFO)-modified electrode (Fig 5 curve b) is much larger than that of the unmodified GCE (Fig 5 curve a), indicating high specific capacitance of poly(SFO) films on electrode. The poly(SFO)-modified GCE facilitated electron transfer rate of the electrooxidation reaction of DA and UA. The safranin O self-assembled monolayers modified electrode showed high electrocatalytic activity toward the oxidation of DA and UA.

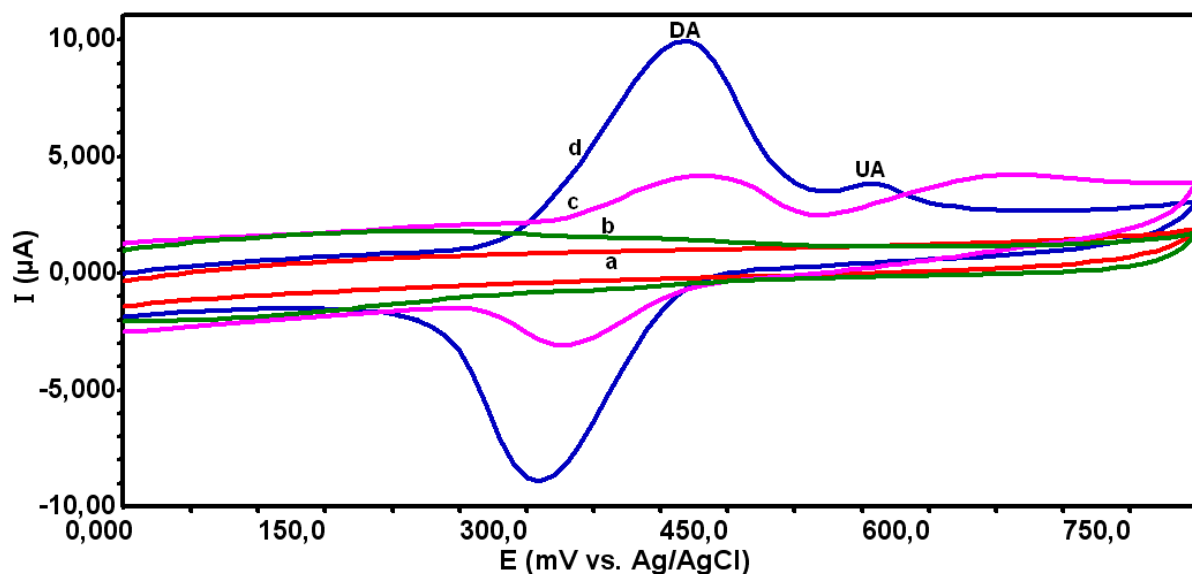


**Figure 5.** CV responses of GCE(c) and poly(SFO)/GCE(d) in 0.1 M acetate buffer solution (pH=4.0). GCE(a) and poly(SFO)/GCE(b) without DA and UA. 0.1 mM [DA] and [UA]. Scan rate was  $50 \text{ mV s}^{-1}$ .

## 3.4. Effect of scan rate

The effect of scan rate on the current response of DA and UA were studied separately. The cyclic voltammograms of DA, and UA at poly(SFO)-modified electrode were carried out at different scan rates. It can be seen that both the peak potentials ( $E_{pa}$ ) and peak currents ( $I_{pa}$ ) are dependent on the scan rate.

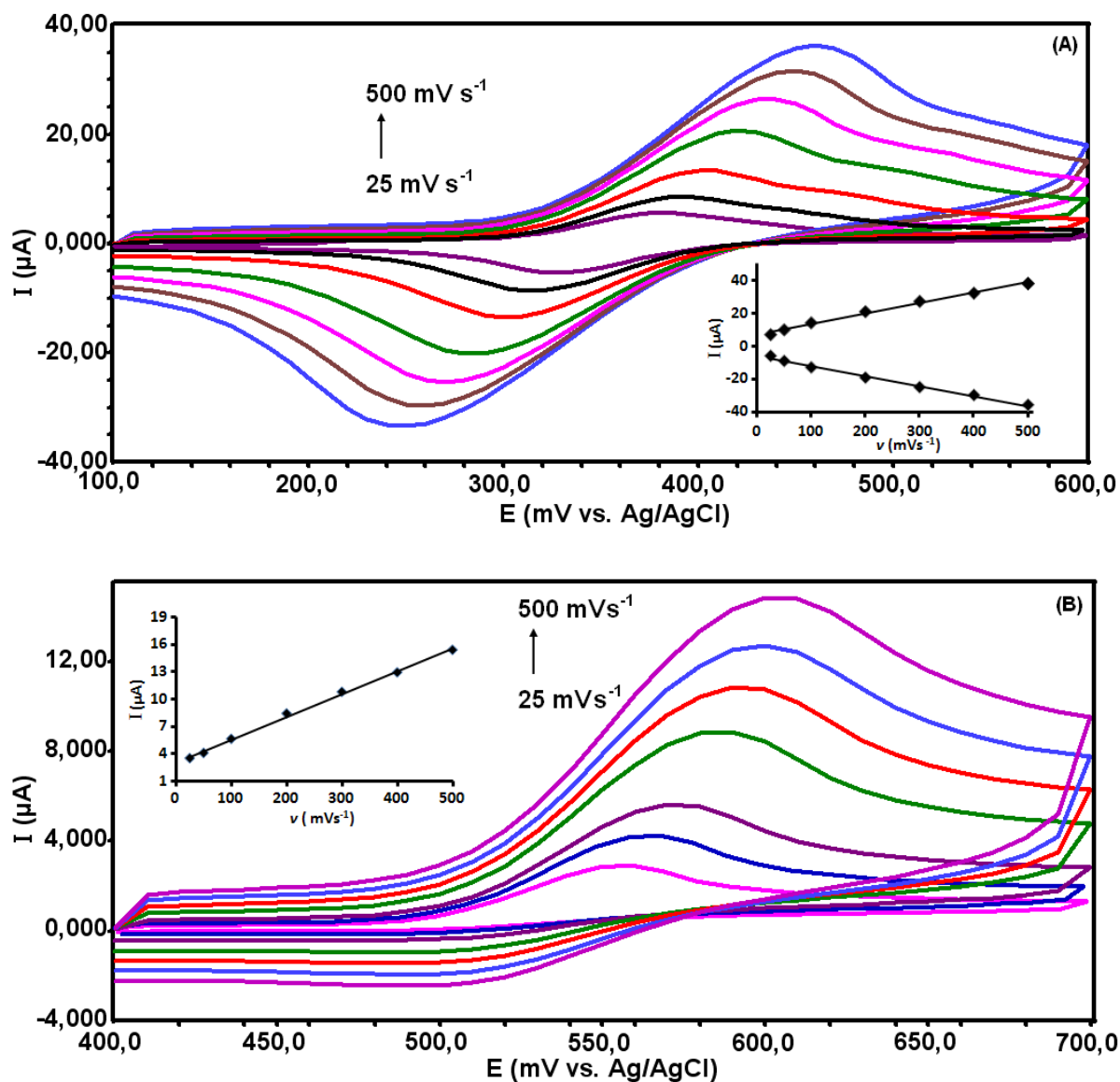


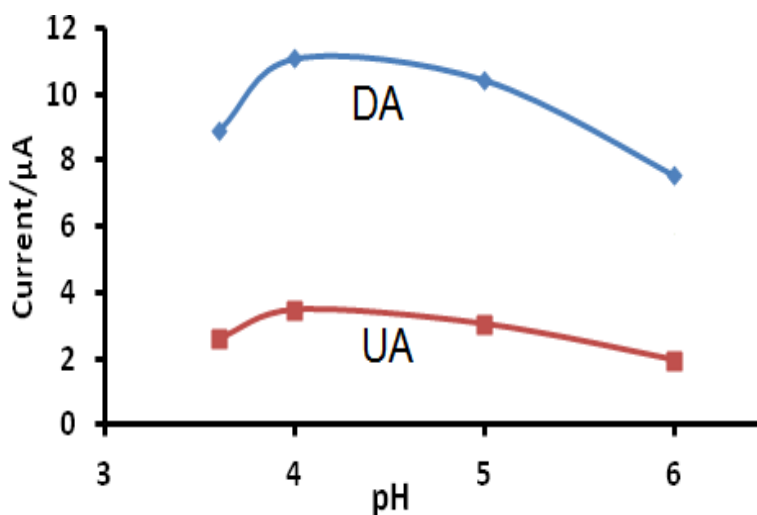
**Figure 6.** Cyclic voltammograms (CVs) of poly(SFO)/GCE in 0.1 M acetate buffer solution containing 0.1 mM DA (A), and 0.1 mM UA (B) at different scan rates of 25, 50, 100, 200, 300, 400, and 500  $\text{mV s}^{-1}$ . Insets: plots of oxidation currents versus the scan rates of DA and UA, respectively.

Test results indicate that there is a linear relationship between the peak current ( $I_{pa}$ ) and the scan rate ( $v$ ) in the range of 25–500  $\text{mV s}^{-1}$ . The linear equations are expressed as follows:  $I_{(pa)} =$

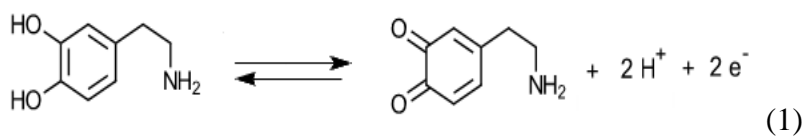
$0.0642 \nu + 6.5862$  ( $R = 0.9918$ ) and  $I_{(pa)} = 0.0251 \nu + 3.0407$  ( $R = 0.9975$ ), for DA and UA, respectively. The results are depicted in Fig. 6 (A and B). The plots of the oxidation peak current as a function of the scan rate was shown as an inset in each Figure. In all two cases, a very good linear relationship between the peak current and the potential scan rate were observed. The oxidation peak potentials of DA and UA were shifted to more positive values with increasing scan rate. The above results indicate that the process for all the two species were the adsorption-controlled process at the modified electrode surface. By plotting  $E_p$  versus  $\log \nu$ , two linear relationships were observed with the linear equations:  $E_{pa}$  (mV) =  $50.161 \log \nu + 307.48$  ( $R = 0.9936$ );  $E_{pc}$  (mV) =  $-45.344 \log \nu - 390.87$  ( $R = 0.9998$ ). According to the Laviron's theory : A graph of  $E_p = f(\log \nu)$  yields two straight lines with a slope equal to  $-2.3 RT/\alpha nF$  for the cathodic peak, and  $2.3RT/(1 - \alpha)nF$  for the anodic peak. The electron transfer coefficient  $\alpha$  could be calculated to be 0.53.

### 3.5. Effect of pH on the oxidation of DA and UA

The effect of solution pH on the peak currents and peak potentials of DA and UA oxidation were investigated. Fig. 7 (inset) shows the changes of the peak currents ( $I_{pa}$ ) of oxidation of DA and UA with pH. The maximum separation of peak potentials for DA–UA is observed at pH 4.0. In order to obtain high sensitivity and selectivity, pH 4.0 was selected as an optimum pH value for the detection of DA and UA in their mixture. Within the pH ranges of 3.6 to 4.0, the anodic peak current of DA and UA increased gradually from the pH of 3.6 to 4.0 and then decreased to pH=6.0. The curve of  $I_p$  vs. pH showed a maximum at pH ca. 4.0 and the response gradually decreased as the pH increased.



**Figure 7.** Effect of pH on the peak current(CV) for the oxidation of 0.1 mM DA and 0.1 mM UA in 0.1 M acetate buffer solution. Scan rate was  $50 \text{ mV s}^{-1}$ .



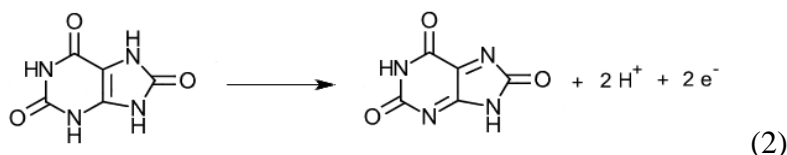


**Figure 8.** Oxidation reaction of DA (1) and UA (2).

In order to achieve high sensitivity, pH=4.0 was chosen for the simultaneous determination of DA and UA. When the pH of a solution was increased, the peak potentials of DA and UA shifted towards more negative potentials. As shown in Fig. 6, UA display irreversible oxidation peaks at 0.555 V. In the case of DA (Fig. 7), the oxidation and reduction peak potentials appear at 0.417 and 0.311 mV (vs. Ag/AgCl, KCl, 3.0 M, pH=4.0), respectively, and the poly(SFO)-modified electrode shows a significantly better reversibility for DA. The equations for peak potential as a function of pH are  $E_{pa} = 670 - 66 \text{ pH}$  (mV,  $R = 0.9961$ ) and  $E_{pa} = 839 - 67 \text{ pH}$  (mV,  $R = 0.9927$ ), for DA and UA, respectively. These slopes are close to a Nernst equation, defined as  $-59 \text{ mV/pH}$  at  $25 \text{ }^\circ\text{C}$ . These results were agreement with the Nernst equation for a two-electron and two-proton transfer reaction (Fig. 8).

### 3.6. Stability, reproducibility, and repeatability of poly(SFO)

To estimate the fabrication reproducibility of the poly(SFO)-modified electrode, the relative standard deviations (% RSD) of five electrodes prepared independently for measuring  $1.0 \text{ } \mu\text{M}$  DA and  $1.0 \text{ } \mu\text{M}$  UA were calculated to be 3.78 % and 3.70 % respectively, indicating good fabrication reproducibility. Measurement repeatability of the poly(SFO)-modified electrode was tested and the relative standard deviation (% RSD) of the peak currents for 10 repetitive assays of  $1.0 \text{ } \mu\text{M}$  DA and  $1.0 \text{ } \mu\text{M}$  UA using SW-AdSV were found to be 4.2 % and 3.8 %, respectively. The experimental results showed that the poly(SFO) has higher reproducibility. The stability of the poly(SFO)-GCE was investigated by keeping the electrode in acetate buffer solution (pH 4.0) for 10 days and then recording the SW-AdSVs for  $1.0 \text{ } \mu\text{M}$  DA and  $1.0 \text{ } \mu\text{M}$  UA, and comparing them with the SW-AdSVs obtained in the same solution before immersion. The results indicates that peak current decreases only slightly for the poly(SFO), indicating that the poly(SFO) modified electrode has good stability.

### 3.7. Optimization of SW-AdSV parameters

The adsorptive stripping peak currents were obtained under different pHs, pulse sizes, frequencies, accumulation potentials, and times. The highest stripping peak currents were obtained at pH 4.0 similar to those found in cyclic voltammetric experiments. The effect of the amplitude on the stripping peak currents was also studied from 50 mV up to 100 mV. As can be seen from Fig. 9(a), as the amplitude increased from 50 mV to 75 mV, the stripping peak currents of DA and UA increased gradually and remained nearly constant. The influence of step size was studied in the range from 5 to 10 mV. As can be seen in Fig. 9(b), the stripping peak current (DA and UA) increased with the step size up to 8 mV. Increasing the step size value beyond 8 mV, gave the sensor with a slightly reduced

response. Therefore, a step size of 8 mV was selected for the rest of the experiments. Varying the value of square wave frequency also plays an important role for the measured signal of SW-AdSV approach. The dependence of the peak intensity on the frequency was tested from 5 Hz to 50 Hz. As can be seen in Fig 9 (c), maximum peak current was observed at 10 Hz. As the frequency increased above 10 Hz, the peak current decreased and the peak was broadened. A frequency of 10 Hz was thus selected for further measurements. The influence of accumulation time and accumulation potential on the electrode response was investigated by SW-AdSV. The effect of accumulation potential on the stripping peak current of DA and UA was examined individually over the potential range of -0.5 V to +0.5 V. The results were depicted in Fig. 9 (d). The experimental results indicated that the highest efficiency of the accumulation of DA and UA was obtained when the accumulation potential was equal to -0.3 V and remained almost constant up to -0.1 V. The guest DA and UA molecules can be accumulated by the immobilized poly(SFO) host as a mediator. When the accumulation potential was more positive than -0.1 V, the adsorptive stripping peak currents of both compounds decreased gradually. An accumulation potential -0.2 V was established for further SW-AdSV studies. The effect of the deposition time on the stripping peaks current was also studied from 100 s up to 600 s. The stripping peak currents of DA and UA increased significantly with the increase of the accumulation time, and reached a maximum at 300 s. Then, the peak currents increased slightly when the time exceeded 300 s. Therefore, this value was selected as the optimal accumulation potential for further measurements.

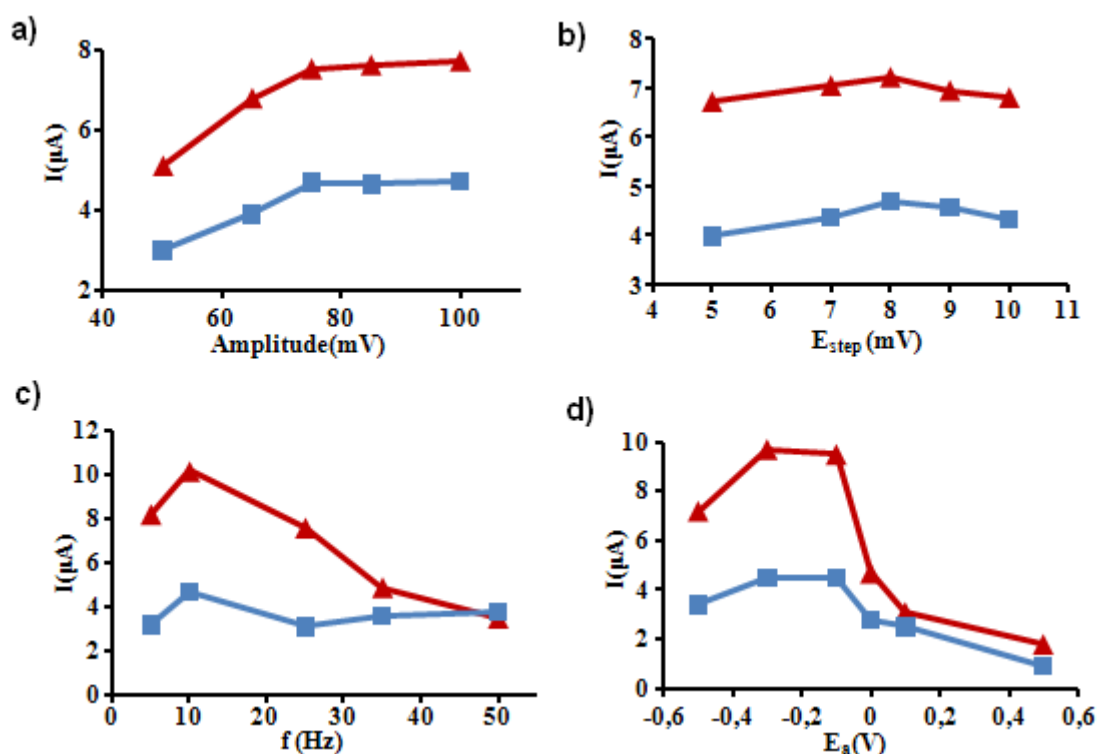


**Figure 9.** Dependence of the SW-AdSV peak current of dopamine ( $\blacktriangle$ ) (10  $\mu\text{M}$ ), uric acid ( $\blacksquare$ ) (10  $\mu\text{M}$ ) on: (a) the amplitude (b) the step size (a) the frequency and (d) the accumulation potential.

## 3.8. Square wave adsorptive stripping voltammetry

SW-AdSVs were carried out in the potential range of 0.2 to 0.7 V. Two well-separated oxidation peaks at about 367, and 540 mV vs Ag/AgCl ( $\text{KCl}, 3.0 \text{ mol L}^{-1}$ ) appears, corresponding to the SW-AdSVs of DA and UA, respectively. Separation of anodic peaks of 176 mV allows us to determine DA and UA simultaneously by using SW-AdSV. The preconcentration processes of DA and UA in the mixture are evaluated when the concentration of one species changes and the other one keeps constant.

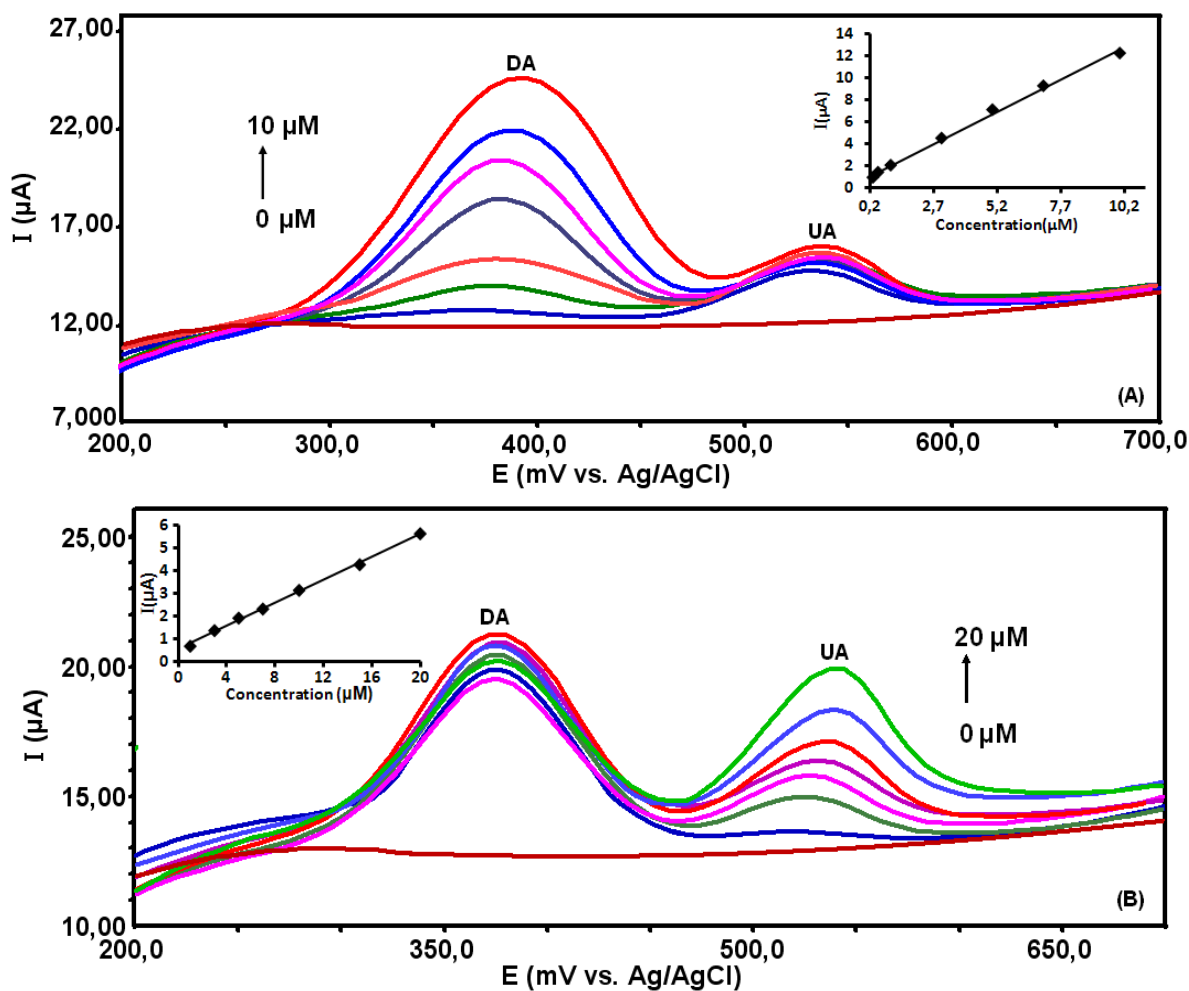


**Figure 10.** (A). Square wave adsorptive stripping voltammograms of DA at poly(SFO) modified GCE in the presence of  $5.0 \mu\text{M}$  UA in acetate buffer, pH 4.0. DA concentrations (from 0.0 to 10): 0.0, 0.3, 0.5, 1.0, 3.0, 5.0, 7.0 and  $10 \mu\text{M}$ . Inset: plot of oxidation current versus DA concentration. (B). Square wave stripping voltammograms of UA at poly(SFO) in the presence of  $5.0 \mu\text{M}$  UA in acetate buffer, pH 4.0. UA concentrations (from 0 to 20): 0.0, 0.5, 3.0, 5.0, 7.0, 10, 15 and  $20 \mu\text{M}$ . Inset: plot of oxidation current versus UA concentration.

Fig. 10 (A) depicts the SW-AdSV curves of various DA concentrations at poly(SFO)/GCE in presence of  $5.0 \mu\text{M}$  UA. As shown in Fig. 10 (A), the oxidation currents of UA show small change

when DA concentration increases; it indicates that the addition of UA does not affect the determination of DA. The corresponding linear regression equation is defined as  $I_p (\mu\text{A}) = 1.1729 C (\mu\text{M}) + 0.2365$  ( $R = 0.9965$ ), and the detection limit for DA was found to be  $0.05 \mu\text{M}$ . Meanwhile, a similar experiment was conducted with UA in the presence of  $5.0 \mu\text{M}$  DA. As can be seen in Fig 10 (B), the oxidation currents of DA show small change when UA concentration increases; it indicates that the addition of DA does not affect the determination of UA. The corresponding linear regression equation is defined as  $I_p (\mu\text{A}) = 0.4978 C (\mu\text{M}) + 0.1454$  ( $R = 0.9978$ ), and the detection limit for UA was observed to be  $0.09 \mu\text{M}$ . The limit of detection, defined as  $C_L = 3S_{y/x}/b$  (where  $S_{y/x}$  is the standard deviation of y-residuals and  $b$  is the slope of the calibration plot). To evaluate the reproducibility of modified electrode, poly(SFO)/GCEs were investigated by comparing the peak currents in  $5 \mu\text{M}$  DA and  $5 \mu\text{M}$  UA in  $0.1 \text{ M}$  PBS (pH 4.0). The relative standard deviation (R.S.D) for DA and UA were 2.5 % and 3.5 %, respectively.

### 3.9. Interference study

The test about the influence of various interferents that may exist in the real samples on the determination of DA and UA was also carried out. It was found that a 100-fold excess of bilirubin, 250-fold excess citric acid, 250-fold excess glutamic acid, 150-fold excess of glucose, 500-fold excess of NaCl, 240-fold excess of  $\text{NaNO}_3$ , 140-fold excess of oxalic acid and 200-fold excess of  $\text{CaCl}_2$  did not interfere with the determination of DA and UA. It is well known that AA widely coexists with DA and UA in real biological matrices. Therefore, it becomes a major goal to selectively detect dopamine and uric acid in the presence of high concentration of ascorbic acid. The poly(SFO) film-coated electrode was tested for simultaneous determination of DA and UA in the presence of large amount of AA by using SW-AdSV technique. It was found that a 2000-fold excess of ascorbic acid did not interfere with the simultaneous determination of DA and UA. The tolerance limit was defined as the maximum concentration of the interfering substance that causes an error of less than 5% for the determination of DA and UA.

### 3.10. Sample analysis

In order to evaluate the applicability of the proposed method for the simultaneously determination of DA and UA in real urine samples, the utility of the proposed method was tested by analysis of these compounds in mixed synthetic and in real samples using standard addition methods. The human urine samples were collected in our laboratory from healthy volunteers. All samples were diluted with acetate buffer (pH 4.0) and appropriate amounts (10 mL) of these diluted urine samples were transferred to the electrochemical cell for the detection of each species using SW-AdSV. The recovery of the SW-AdSV method was also investigated to evaluate the accuracy of the method, and the results are listed in Table 1. The recoveries of DA and UA were in the range from 96 % to 103%. The good recoveries of the mixture samples point to the successful applicability of the proposed method to simultaneous determination of DA and UA.

#### 4. CONCLUSION

The proposed method is useful and suitable for the simultaneous electrochemical preconcentration and determination of dopamine and uric acid in real samples by means of square wave adsorptive stripping voltammetry (SW-AdSV). The poly(SFO) modified GCE was shown to have good electrochemical catalytic activity to the reactions studied by considerably decreasing the over-potential of the oxidation reactions studied. Its surface reproducibility was satisfactory, and it has a long-term stability. The results suggest that square wave adsorptive stripping voltammetric determination of DA and UA in biological fluids are free of interference from other common substances.

#### ACKNOWLEDGEMENTS

We gratefully acknowledge Istanbul University Scientific Research Fund (Project No. BYP-20075 and UDP-26215) for financial support.

#### References

1. R. M. Wightman, L. J. May, A. C. Michael, *Anal. Chem.* 60 (1988) 769A-779A.
2. X. W. Wu, D. M. Muzny, C. C. Lee, C. T. Caskey, *J. Mol. Evol.* 34 (1992) 78-84.
3. M. Oda, Y. Satta, O. Takenaka, N. Takahata, *Mol. Biol. Evol.* 19 (2002) 640-653.
4. R. J. Johnson, D. H. Kang, J. R. Cade, B. A. Rideout, W. J. Oliver, *Semin. Nephrol.* 25 (2005) 3-8.
5. E. Visser, P. R. Bär, H. A. Jinnah, *Brain Res. Rev.* 32 (2000) 449-75.
6. J. Zen, P. Chen, *Anal. Chem.* 69 (1997) 5087-5093.
7. X. Liu, Y. Peng, X. Qua, S. Ai, R. Han, X. Zhu, *J. Electroanal. Chem.* 654 (2011) 72-78.
8. S. Shahrokhian, H. R. Zare-Mehrjardi, *Sens. Actuators B* 121 (2007) 530-537.
9. K. C. Lin, C. Y. Yin, S. M. Chen, *Int. J. Electrochem. Sci.* 6 (2011) 3951-3965.
10. A. A. Ensafi, M. Taei, T. Khayamian, *Int. J. Electrochem. Sci.* 5 (2010) 116-130.
11. D. Deletioğlu, E. Hasdemir, A.O. Solak, *Curr. Anal. Chem.* 6(3) (2010) 203-208.
12. D. Zheng, J. Ye, L. Zhou, Y. Zhang, C. Yu, *J. Electroanal. Chem.* 625 (2009) 82-87.
13. S. Shahrokhian, M. Ghalkhani, *Electrochim. Acta* 51 (2006) 2599-2606.
14. M. Noroozifar, M. Khorasani-Motlagh, A. Taheri, *Talanta* 80 (2010) 1657-1664.
15. J. Huang, Y. Liu, H. Hou, T. You, *Biosens. Bioelectron.* 24 (2008) 632-637.
16. Y. Liu, J. Huang, H. Hou, T. You, *Electroanal. Chem.* 10 (2008) 1431-1434.
17. X. Niu, W. Yang, H. Guo, J. Ren, F. Yang, J. Gao, *Talanta* 99 (2012) 984-8.
18. C.-L. Sun, H. Lee, J. M. Yang, C. C. Wu, *Biosens. Bioelectron.* 26 (2011) 3450-3455.
19. J. Ping, J. Wu, Y. Wang, T. Ying, *Biosens Bioelectron.* 34 (2012) 70-76.
20. D. Han, T. Han, C. Shan, A. Ivaska, L. Niu, *Electroanalysis* 22 (2010) 2001-2008.
21. R. Cui, X. Wang, G. Zhang, C. Wang, *Sens. Actuators B.* 161 (2012) 1139-1143.
22. R. Akbari, M. Noroozifar, M. Khorasani-Motlagh, A. Taheri, *Anal. Sci.* 26(4) (2010) 425-30.
23. A. Safavi, N. Maleki, O. Moradlou, F. Tajabadi, *Anal. Biochem.* 359 (2006) 224-229.
24. A. A. Ensafi, M. Taei, T. Khayamian, *Int. J. Electrochem. Sci.* 5 (2010) 116-130.
25. H. Yao, Y. Sun, X. Lin, Y. Tang, L. Huang, *Electrochim. Acta* 52 (2007) 6165-6171.
26. J. M. Zen, P. J. Chen, *Anal. Chem.* 69 (1997) 5087-5093.
27. A. Safavi, N. Maleki, O. Moradlou, F. Tajabadi, *Anal. Biochem.* 359 (2) (2006) 224-9.
28. A. Balamurugan, S. M. Chen, *Anal. Chim. Acta* 596 (2007) 92-98.
29. P. Wang, Y. Li, X. Huang, L. Wang, *Talanta* 73 (2007) 431-437.

30. P. Ramesh, S. Sampath, *Electroanalysis* 16 (2004) 866-869.
31. A. A. Ensafi, M. Taei, T. Khayamian, A. Arabzadeh, *Sens. Actuators B* 147 (2010) 213-221.
32. J. Du, R. Yue, F. Ren, Z. Yao, F. Jiang, P. Yang, Y. Du, *Gold Bull.* 46 (2013) 137-144
33. R. C. Prince, S. J. G. Linkletter, P. L. Dutton, *Biochim. Biophys. Acta* 635 (1981) 132-148.
34. A. J. Bard, L. Faulkner, *Electrochemical Methods*, Wiley, New York (2001).
35. J. Wang, *Analytical Electrochemistry* 3rd ed., Wiley-VCH (2006).
36. R. Kalvoda, M. Kopanica, *Pure Appl. Chem.* 61 (1989) 97-112.
37. A. H. Alghamdi, *Arabian J. Chem.* 3 (2010) 1-7.
38. J.-C. Vire, J.-M. Kauffmann, G. J. Patriarche, *J. Pharm. Biomed. Anal.*, 7 (1989) 1323-1335.
39. R. Gulaboski, C. M. Pereira, *Electrochemical Methods and Instrumentation in Food Analysis*, in *Handbook of Food Analysis* (2008) (Semih Ottles, Ed.) Taylor & Francis.
40. G. Ćirić-Marjanović, N. V. Blinova, M. Trchová, J. Stejskal, *J. Phys. Chem. B* 111 (2007) 2188-2199.
41. T. Komura, M. Ishihara, T. Yamaguchi, K. Takahashi, *J. Electroanal. Chem.* 493 (2000) 84-92.
42. T. Komura, T. Yamaguchi, M. Ishihara, G. Y. Niu, *J. Electroanal. Chem.* 513 (2001) 59-66.
43. T. Tanaka, K. Tokuda, T. Ohsaka, *T. J. Chem. Soc., Chem. Commun.* 23 (1993) 1770-1772.
44. T. Selvaraju, R. Ramaraj, *Electrochem. Commun.* 5 (2003) 667-672.
45. V. Ganesan, R. Ramaraj, *J. Appl. Electrochem.* 30 (2000) 757-760.
46. X.-Y. Liu, *Bull. Korean Chem. Soc.* 31 (2010) 1182-1186.
47. L. Niu, K. Lian, W. Kang, S. Li, *J. Braz. Chem. Soc.* 22 (2011) 204-210.
48. R. Pauliukaite, A. Selskiene, A. Malinauskas, C. M.A. Brett, *Thin Solid Films* 517 (2009) 5435-5441.
49. X.-G. Li, M. R. Huang, W. Duan, Y. L. Yang, *Chem. Rev.* 102 (2002) 2925-3030.
50. S. Guo, Q. Zhu, B. Yang, J. Wang, B. Ye, *Food Chem.* 129 (2011) 1311-1314.